Electronic Supporting Information (ESI)

Influence of Water Concentration on the Solvothermal Synthesis of VO_2(B) Nanocrystals

Brittney A. Beidelman, Xiaotian Zhang, Karla, R. Sanchez-Lievanos, Annabel V. Selino, Ellen M. Matson*, and Kathryn E. Knowles*

Department of Chemistry, University of Rochester, Rochester, New York 14627, USA.

*Corresponding author email: matson@chem.rochester.edu, kknowles@ur.rochester.edu

Supporting Information Table of Contents:

Table S1. Previously reported reaction conditions for the synthesis of VO_2 (A) and (B).

V Precursor	Ligands	Solvent	Temperature(°C)/ Time(hrs)	VO_2 phase and Shape	Ref
V_2O_5	2 equiv. $NaHSO_3$	Water	220/24	A, rods, 20 nm diameter and length of 0.1–1 μm	1
V_2O_5	1.5 equiv. oxalic acid	Water	250/24	A, rods, 2-4μm length	2
V_2O_5	1-3 equiv. oxalic acid	Water	230-270/24	A, rods, 2-20μm length	3
V_2O_5	2 equiv. oxalic acid	Water	230/24	A, rods, 5 mm length, 150 nm width	4
V_2O_5	1 equiv. quinol	Water	180/24	B, rod bundles, 2-3μm length, 1μm thick	5
V_2O_5	2 equiv. 4-butylaniline	Water	180/48	B, rods, 2-3μm length, 80nm thick	6
V_2O_5	26 equiv. H_2O_2, 14 equiv. ethanol	Water	180/48	B, rods, 1-3μm length	7
V_2O_5	2 equiv. 2-phenylethylamine	Water	180/48	B, belts, 3-10μm length, 66nm width	8
$VO(acac)_2$	None	Water	220/24	A, nanoplates, 20–40 nm wide and 100–200 nm long	9
$VO(acac)_2$	3.4 equiv. Ethanol	Water	170-220/8-72	A, nanoribbons, 30nm diameter, 2-20μm length	10
$VO(acac)_2$	None	Water	200/12	B, nanoplates, 150nm wide, 300nm long	10
$VO(acac)_2$	4.7 equiv. PVP	Water	200/24	B, nanoflowers, 1-1.5μm diameter	11
$VO(acac)_2$	4 equiv. Lauric acid, 2 equiv. water	Toluene	200/24	A, platelets, 17.8± 6.5nm length/width, 4.5±1.2nm thick	This work
$VO(acac)_2$	4 equiv. Lauric acid, 20 equiv. water	Toluene	200/24	B, nanorods, 13.1±5.4nm width, 75.4±29.9nm length	This work

Experimental Details of the Powder X-ray Diffraction Measurements

Powder samples were affixed to a Nylon loop (0.1 mm ID) with a light coating of viscous oil and mounted on a goniometer. X-ray diffraction data were collected on a Rigaku XtaLAB Synergy-S diffraction system equipped with a HyPix-6000HE HPC detector. Cu Kα radiation (λ = 1.54184 Å) and Mo Kα radiation (λ = 0.71073 Å) were generated by PhotonJet-S microfocus sources operated at 50 kV, 1 mA. Each data set was collected at room temperature. For each scan, φ was rotated through 720° in 300 s (2.4°/s). The sample-to-detector distance and w, q, and k angles were fixed and optimized for each sample. Table S2 summarizes the parameters used for the spectra shown in Figure 1C in the main text.

Table S2. Parameters used to collect Powder X-ray Diffraction Spectra

	2 equiv. H_2O[a,c]	4 equiv. H_2O[b]	12 equiv. H_2O[a]	20 equiv. H_2O[a]
Sample-to-detector distance	33.2 mm	34.0 mm	34.0 mm	33.2 mm
ω	scan 1: -41.25° scan 2: 40.47°	-13.02°	-41.95°	-41.18°
θ	scan 1: -41.25° scan 2: 40.47°	-13.02°	-41.95°	-41.18°
κ	scan 1: 0° scan 2: 0°	0°	0°	0°

[a]Collected using Cu Kα radiation, λ = 1.54184 Å. [b]Collected using Mo Kα radiation, λ = 0.71073 Å [c]Spectrum reported in Figure 1C is the average of two scans.

In order to compare the peak positions observed in the spectrum collected with Mo Kα radiation to those observed in the spectrum collected with Cu Kα radiation, we converted the 2θ values obtained from the Mo Kα collection ($2\theta_{Mo}$) to those consistent with Cu Ka radiation ($2\theta_{Cu}$) using eq. S1, where λ_{Cu} = 1.54184 Å and λ_{Mo} = 0.71073 Å.

$$\sin\theta_{Cu} = \lambda_{Cu}\frac{\sin\theta_{Mo}}{\lambda_{Mo}} \quad \text{(S1)}$$

We note that this converted spectrum was used exclusively for the purposes of phase identification by comparing peak positions to a reference spectrum.

MatLAB code used to model oriented attachment (MatLAB version R2020a):

```
pd=fitdist(rxn_3hrs,'Normal'); %define a probability distribution function
                               %based on a fit of the size distribution
                               %collected after 3 hours of reaction to a
                               %Normal distribution
rng('shuffle')                 %initiate random number generator
r=random(pd,10000,1);          %construct a column vector containing 10000
                               %random numbers generated using the
                               %probability distribution function pd.
                               %This is our model distribution.

r=abs(r);                      %ensure all numbers are positive

for c = 1:2000
    s=size(r);
    n=randperm(s(1),2);    %generate two random integers between 1 and the
                           %number of entries in the model distribution of
                           %rod lengths (r)
    new=r(n(1))+r(n(2));   %create a new entry for the model distribution
                           %equal to the sum of two randomly chosen entries
    r(n(1))=[];            %delete the randomly chosen entries from the
    if n(1) < n(2)         %model distribution
        r(n(2)-1)=[];
    else
        r(n(2))=[];
    end
    r=cat(1,r,new);      %add the new entry to the distribution
end
```

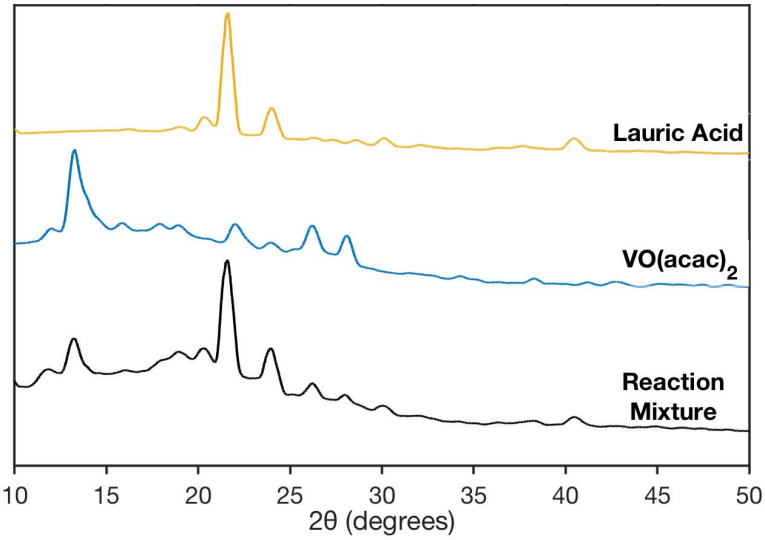

Figure S1. Powder X-ray diffraction spectra of the solid recovered from a reaction mixture containing 0.25 mmol of $VO(acac)_2$ and 1.0 mmol of lauric acid in dry toluene after heating to 200 °C for 24 hours (black), $VO(acac)_2$ (blue), and lauric acid (yellow). The diffraction peaks observed in the reaction mixture correspond to $VO(acac)_2$ and lauric acid.

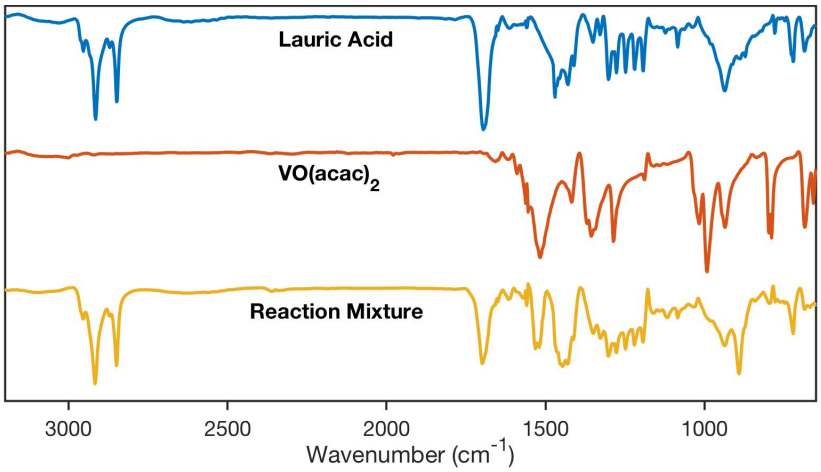

Figure S2. Fourier-transform infrared spectrum of the solid recovered from a reaction mixture containing $VO(acac)_2$, lauric acid, and dry toluene after heating at 200 °C for 24 hours (yellow). FTIR spectra of lauric acid (blue) and $VO(acac)_2$ (red) are included for comparison. All of the peaks observed in the post-reaction mixture can be accounted for in the starting materials.

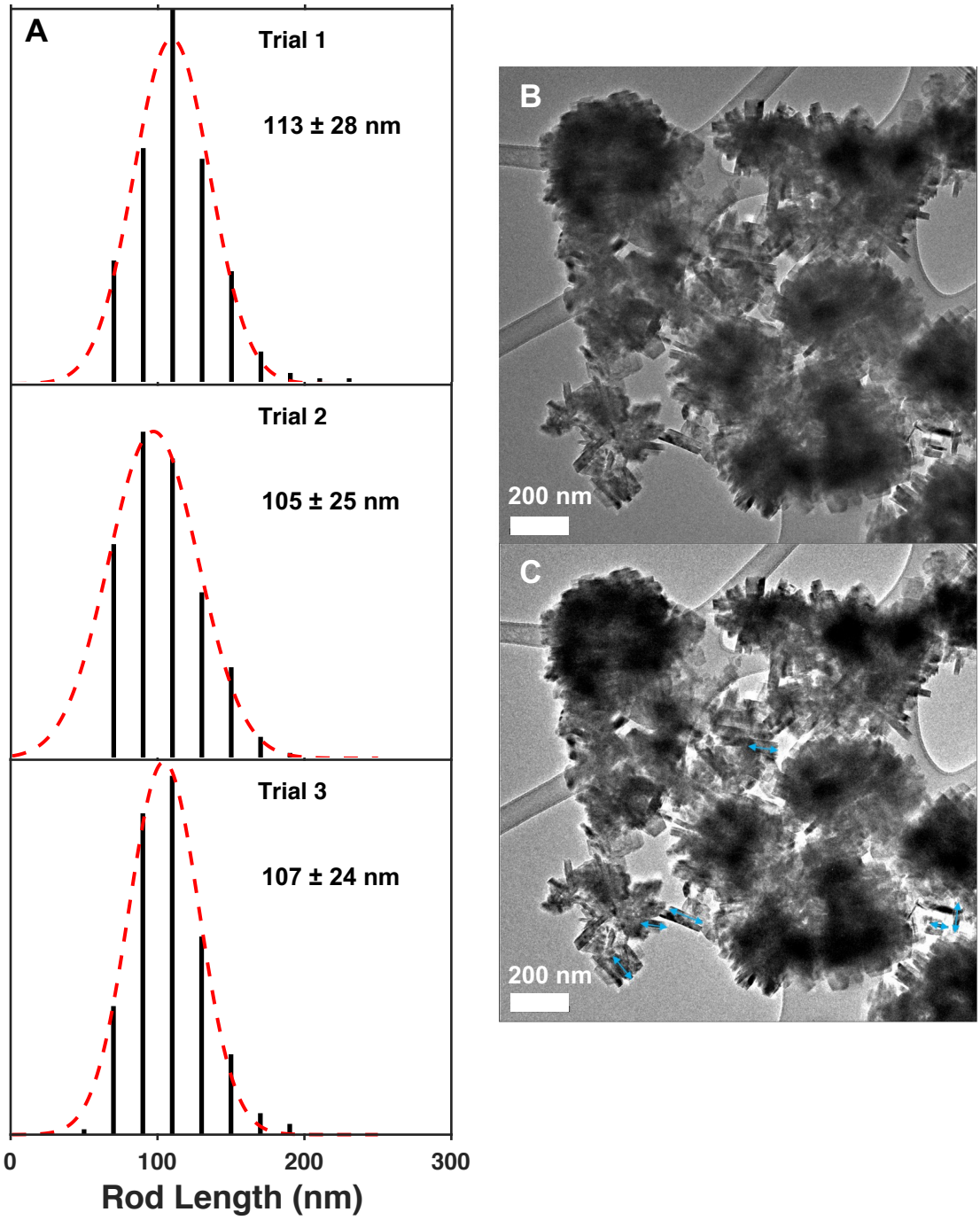

Figure S3. A) Histograms tabulating the lengths of VO_2(B) nanorods measured by TEM for three different reactions run under the same conditions: $VO(acac)_2$ in the presence of 4 equivalents of lauric acid and 20 equivalents of water per vanadium centre. The dashed red lines represent Gaussian fits to the data and each plot is labeled with the average and standard deviation of the data set. **B,C)** Representative TEM images illustrating how the lengths of VO_2(B) nanorods were measured. The image shown in part **C** was produced by increasing the contrast of the image in part B by 5%. Increasing the contrast improves the visibility of the edges of the nanocrystals and enables measurement of the nanorod lengths indicated by the blue double-headed arrows.

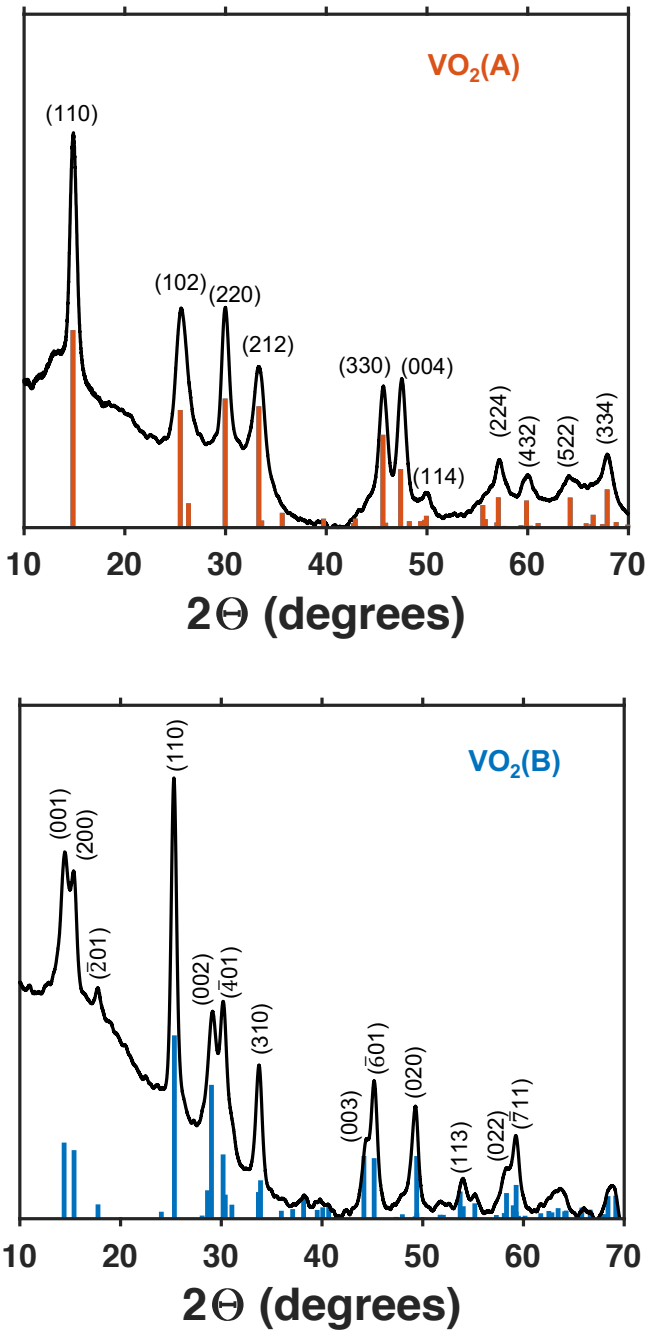

Figure S4. Indexed powder X-ray diffraction patterns for VO_2(A) (top, orange) and VO_2(B) (bottom, blue). The experimental spectra, plotted in black, are obtained from reactions of $VO(acac)_2$ in the presence of 2 equivalents (top) and 20 equivalents (bottom) of water. The vertical bars plot the standard patterns obtained from the JCPDS data base. VO_2(A): JCPDS 00-042-0876, VO_2(B): JCPDS 01-081-2392.

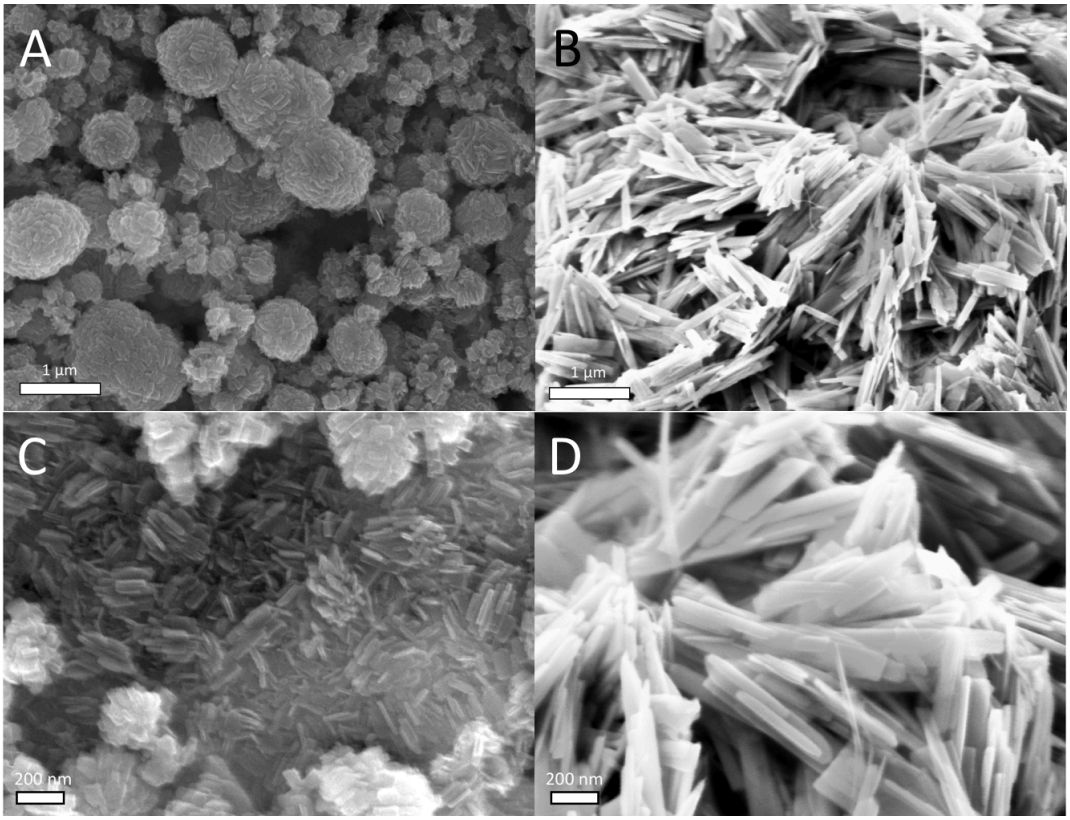

Figure S5. Scanning electron microscope images of VO_2(B) nanobelts obtained from the reaction of $VO(acac)_2$ in toluene containing 20 equivalents of water (A, C) and the reaction of $VO(acac)_2$ in pure water (B, D). The scale bars in A, B correspond to 1 µm and the scale bars in C, D correspond to 200 nm.

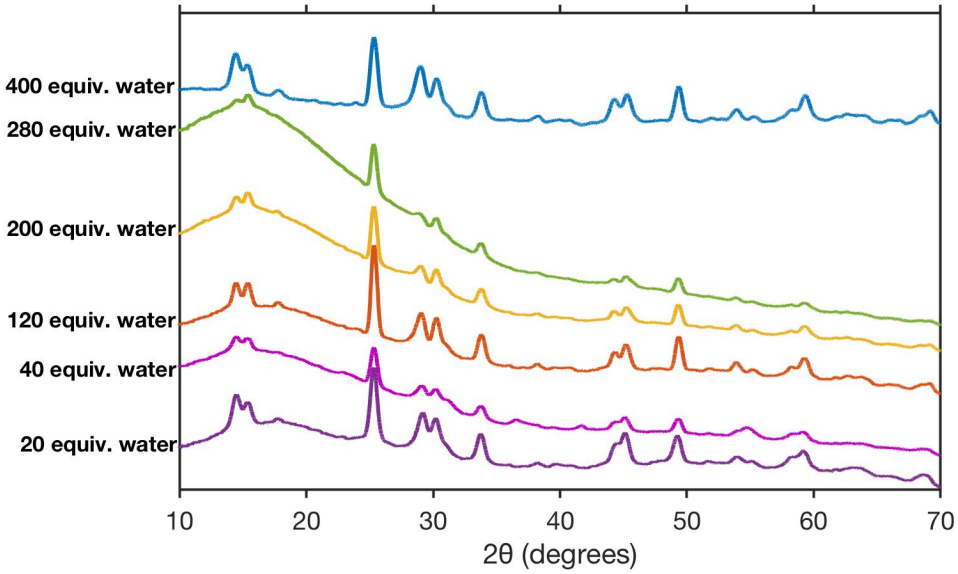

Figure S6. Powder X-ray diffraction spectra of nanocrystal products isolated from reaction mixtures containing $VO(acac)_2$, four equivalents of lauric acid, and 20-400 equivalents of water. All of these reactions produced phase-pure VO_2(B) (JCPDS card no. 01-081-2392).

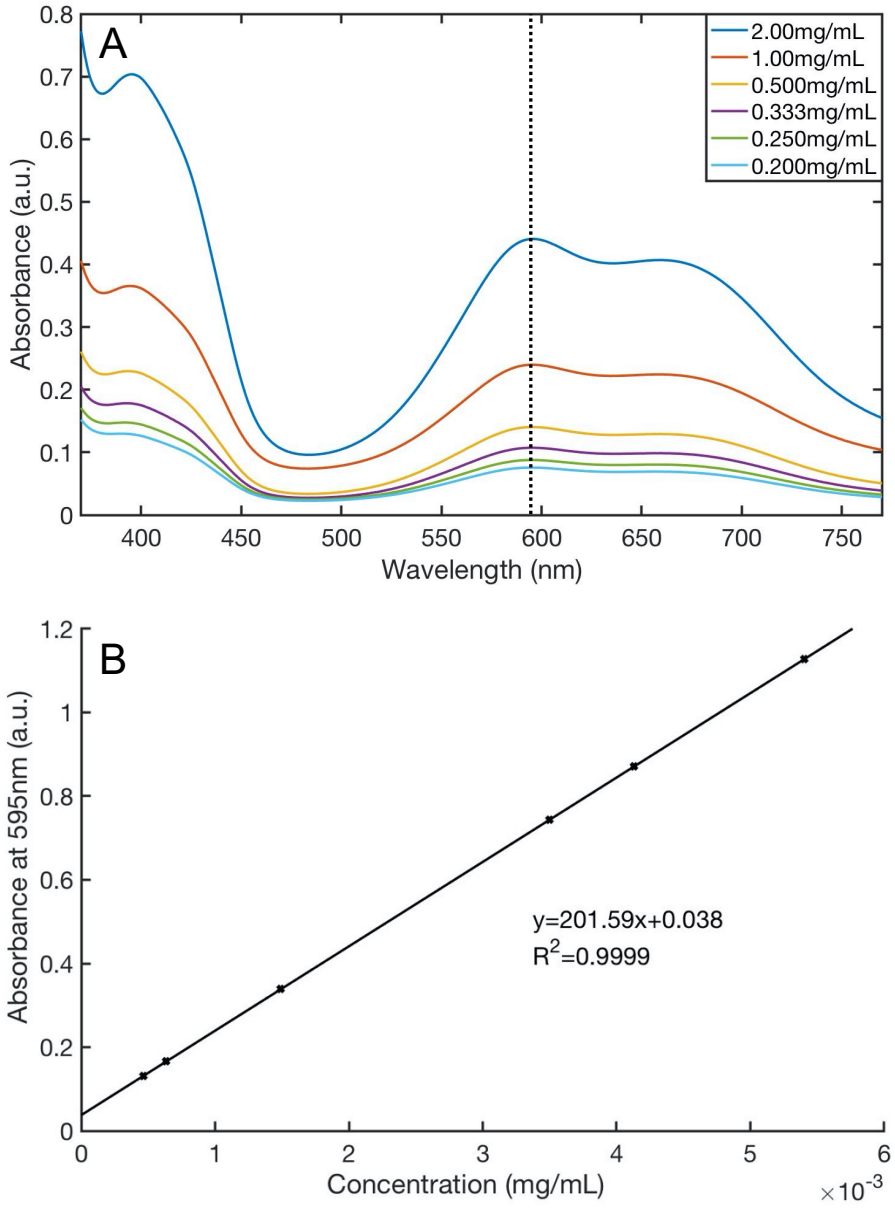

Figure S7. A) Electronic absorption spectra of solutions containing various concentrations of $VO(acac)_2$ in toluene measured in a 1-cm cuvette. The dotted black line indicates the wavelength at which the molar extinction coefficient was determined (λ = 595 nm). The concentrations used were 2.00mg/mL, 1.00mg/mL, 0.500mg/mL, 0.333mg/mL, 0.250mg/mL, and 0.200mg/mL. These concentrations were obtained by serial dilutions of a stock solution with a concentration of 2.00mg/mL. **B)** Plot of absorbance at 595 nm extracted from the spectra shown in part **A** versus the concentration of VO(acac)2 in toluene. A linear fit of these data produces a slope of 201.6 mL/mg, which coresponds to an extinction coefficient of ε_{595} = 53460 M^{-1} cm^{-1}. The y-intercept corresponds to a small constant offset present in all of the spectra.

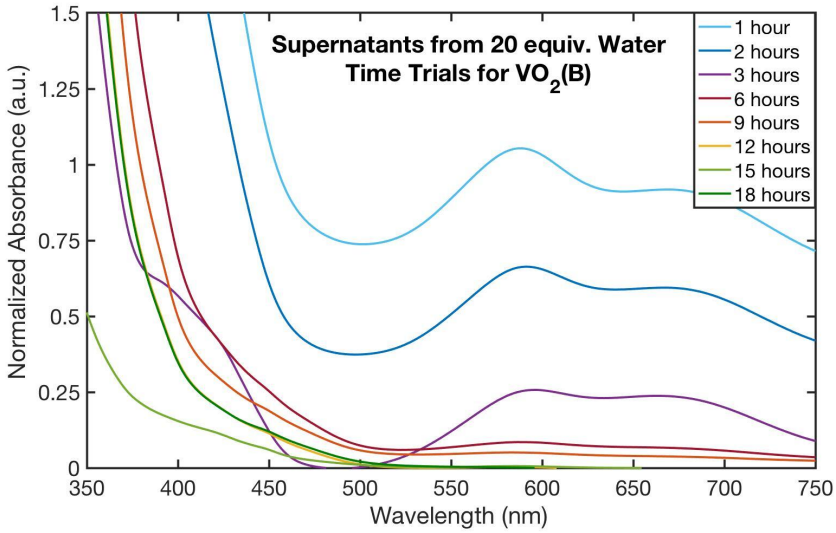

Figure S8. Electronic absorption spectra of supernatants collected from reactions run for various durations ranging from 1 - 18 hours in the presence of 20 equivalents of water.

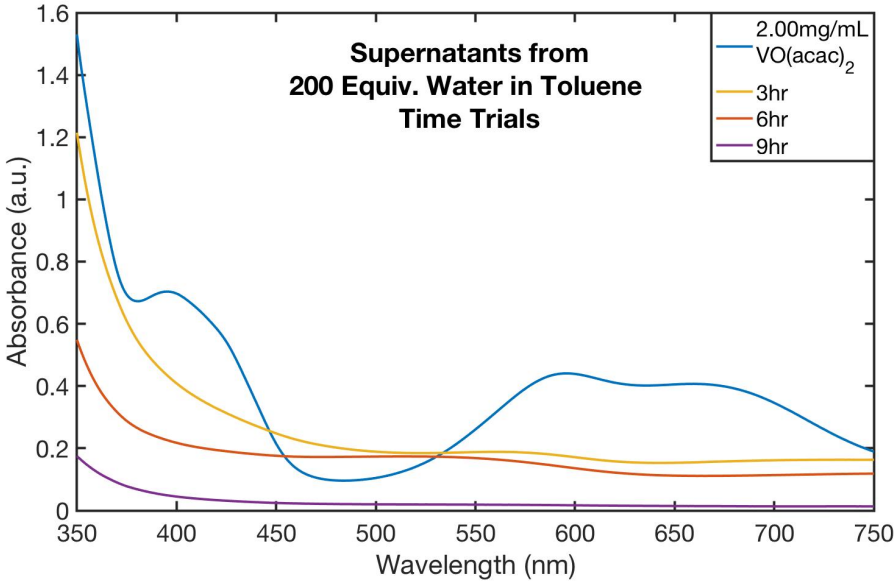

Figure S9. Electronic absorption spectra of supernatants collected from reactions run for 3 (orange), 6 (red), and 9 (purple) hours in the presence of 200 equivalents of water. A spectrum of a solution containing 2.00 mg/mL of VO(acac)2 in toluene is plotted in blue for reference.

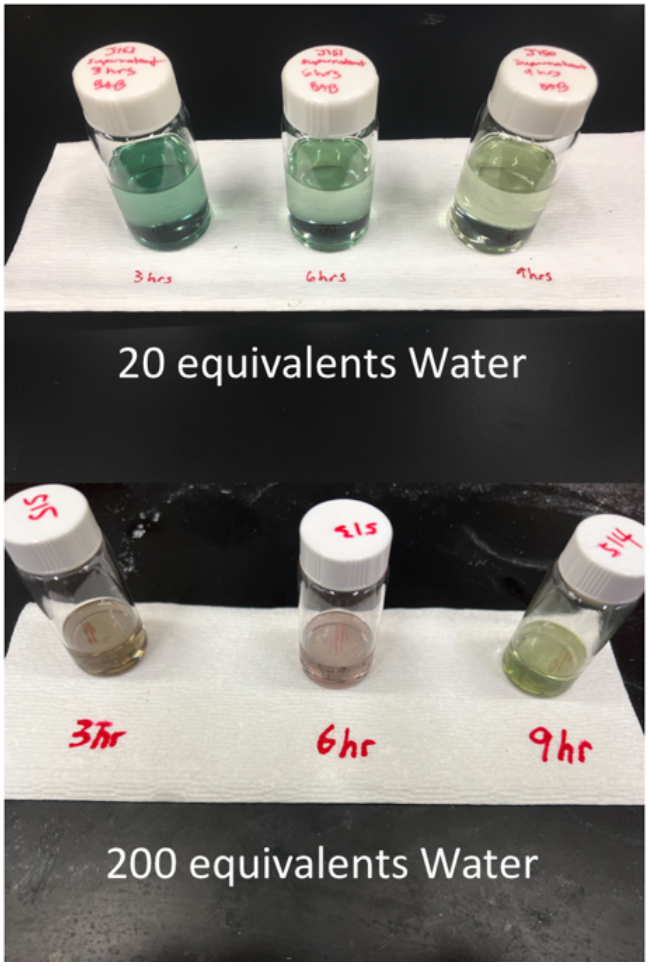

Figure S10. Photographs of supernatant solutions corresponding to the electronic absorption spectra plotted in figures S8 (top) and S9 (bottom). These samples contain solids recovered from rotovapped supernatant solutions that were subsequently redispersed in 10 mL of toluene and filtered. The blue-green color in the 3 and 6 hour samples run with 20 equivalents of water is characteristic of $VO(acac)_2$. The brown color in the corresponding reaction times for 200 equivalents of water is consistent with incomplete separation of nanoparticle products from the supernatant.

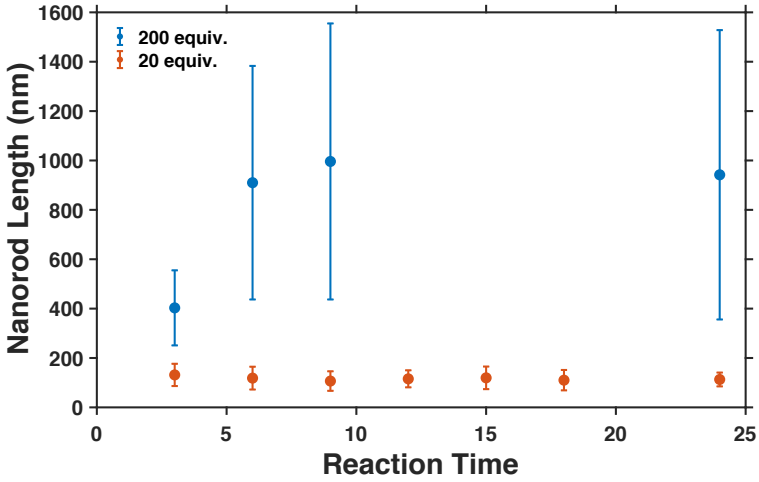

Figure S11. Plot of the average length of VO_2(B) nanorods versus reaction time. The reaction mixtures contained $VO(acac)_2$, 4 equivalents of lauric acid, and 20 (orange) or 200 (blue) equivalents of water in 10 mL of toluene. Each data point represents the average and standard deviation of 210 nanorod lengths measured via analysis of TEM images using ImageJ software.

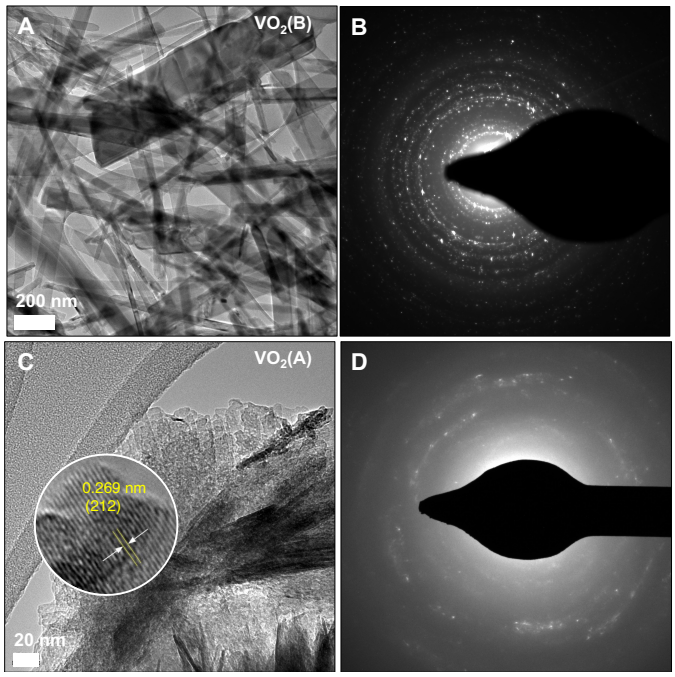

Figure S12. A) TEM image of VO_2(B) nanorods obtained upon reaction of $VO(acac)_2$ with 200 equivalents of water for 24 hours. B) Selected area electron diffraction of the nanorods shown in **A**. **C**) TEM image of VO_2(A) nanocrystals obtained upon reaction of $VO(acac)_2$ with 2 equivalents of water for 24 hours. Inset: High resolution TEM image in which the d-spacing for the (212) plane is resolved. **D**) Selected area electron diffraction of the nanocrystals shown in **C**.

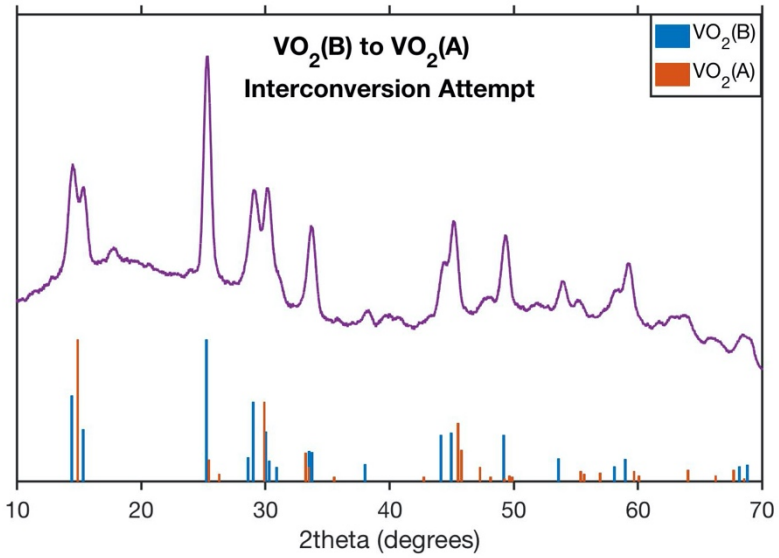

Figure S13. Powder X-ray diffraction spectrum of the nanocrystalline product obtained after reacting VO_2(B) nanocrystals synthesized with 20 equivalents of water under conditions used for synthesizing VO_2(A): 1 mmol lauric acid, 0.5 mmol water, and 10 mL toluene in an autoclave at 200 °C for 24 hours. The reaction yielded VO_2(B), indicating that no phase transformation occurred under these conditions.

References

1. Z. Liangmiao, J. Yao, Y. Guo, F. Xia, Y. Cui, B. Liu and Y. Gao, *Ceram. Int.*, 2018, **44,** 19301-19306.
2. S. Popuri, A. Artemenko, C. Labrugere, M. Miclau, A. Villesuzanne and M. Pollet, *J. Solid State Chem.*, 2014, **213**, 79-86.
3. S. Ji, F. Zhang and P. Jin, *J. Solid State Chem.*, 2011, **184**, 2285-2292.
4. X. H. Cheng, H. F. Xu, Z. Z. Wang, K. R. Zhu, G. Li and S. Jin, *Mater. Res. Bull.*, 2013, **48**, 3383-3388.
5. N. Ganganagappa and A. Siddaramanna, *Mater. Charact.*, 2012, **68**, 58-62.
6. L. Soltane and F. Sediri, *Mater. Res. Bull.*, 2014, **53**, 79-83.
7. Y. Zhang, *Mater. Sci.-Pol.*, 2016, **34**, 169-176.
8. F. Sediri and N. Gharbi, *Mater. Lett.*, 2009, **63**, 15-18.
9. L. Zhang, F. Xia, Z. Song, N. A. S. Webster, H. Luo and Y. Gao, *RSC Adv.*, 2015, **5**, 61371-61379.
10. S. Zhang, B. Shang, J. Yang, W. Yan, S. Wei and Y. Xie, *Phys. Chem. Chem. Phys.*, 2011, **13**, 15873-15881.
11. S. Zhang, Y. Li, C. Wu, F. Zheng and Y. Xie, *J. Phys. Chem. C*, 2009, **113**, 15058-15067.